Available online at www.sciencedirect.com
ScienceDirect
Developmental Biology 303 (2007) 663–674
DEVELOPMENTAL BIOLOGY
www.elsevier.com/locate/ydbio

Runx1 selectively regulates cell fate specification and axonal projections of dorsal root ganglion neurons

Masaaki Yoshikawa [a], Kouji Senzaki [a], Tomomasa Yokomizo [b], Satoru Takahashi [a], Shigeru Ozaki [a], Takashi Shiga [a,*]

[a] *Graduate School of Comprehensive Human Sciences, University of Tsukuba, 1-1-1 Tennodai, Tsukuba 305-8577, Japan*
[b] *Department of Cell Biology and Genetics, Erasmus University, PO Box 1738, 3000 DR Rotterdam, The Netherlands*

Received for publication 28 October 2006; revised 22 November 2006; accepted 4 December 2006
Available online 15 December 2006

Abstract

Runx1-deficient mice die around embryonic day 11.5 due to impaired hematopoiesis. This early death prevents the analysis of the role of Runx1 in the development of sensory ganglia. To overcome the early embryonic lethality, we adopted a new approach to utilize transgenic *Runx1*-deficient mice in which hematopoietic cells are selectively rescued by Runx1 expression under the control of *GATA-1* promoter. In *Runx1*-deficient mice, the total number of dorsal root ganglion (DRG) neurons was increased, probably because of an increased proliferative activity of DRG progenitor cells and decreased apoptosis. In the mutant DRG, TrkA-positive neurons and peptidergic neurons were increased, while c-ret-positive neurons were decreased. Axonal projections were also altered, in that both central and peripheral projections of CGRP-positive axons were increased. In the dorsal horn of the spinal cord, projections of CGRP-positive axons expanded to the deeper layer, IIi, from the normal terminal area, I/IIo. Our results suggest that Runx1 is involved in the cell fate specification of cutaneous neurons, as well as their projections to central and peripheral targets.

Keywords: Runx; Transcription factor; Knockout mouse; Dorsal root ganglion; CGRP; Spinal cord; TrkA; c-ret; Cell-type specification; Axonal projection

Introduction

Runt-related (*Runx*) genes encode the DNA-binding α-subunit of the Runt domain transcription factor, polyomavirus enhancer-binding protein 2 (PEBP2)/core-binding factor (CBF). The Runt-related transcription factors are phylogenetically conserved and play important roles in embryogenesis (for a review, see Coffman, 2003). In *Drosophila*, the *runt* gene regulates various developmental processes including segmentation and neuronal differentiation (Dormand and Brand, 1998; Duffy et al., 1991). In mammals, there are three members of Runx family transcription factors: Runx1, 2 and 3 (Ito, 2004). These transcription factors play critical roles in the development of various cell types from endodermal, mesodermal and ectodermal origin, and mutations in these transcription factors are closely related to specific diseases (De Brujin and Speck, 2004; Stein et al., 2004; Suk-Chul and Joong-Kook, 2004). From these studies, it was determined that Runx1 regulates the differentiation of hematopoietic cells in the fetal liver and its mutation is closely associated with human acute myeloid leukemia. In addition, Runx2 regulates the differentiation of osteoblasts and is associated with cleidocranial dysplasia. Finally, Runx3 regulates the proliferation and survival of gastric epithelial cells and is related to gastric cancer.

Recent studies have shown that Runx1 and Runx3 are also expressed in specific subtypes of neurons in the peripheral and central nervous systems (Inoue et al., 2002; Levanon et al., 2001; Simeone et al., 1995; Theriault et al., 2004). In the dorsal root ganglion (DRG), Runx1 and Runx3 are expressed in the TrkA-expressing ($TrkA^+$) cutaneous neurons and TrkC-expressing ($TrkC^+$) proprioceptive neurons, respectively (Chen et al., 2006a,b; Kramer et al., 2006; Levanon et al., 2001; Marmigere et al., 2006). This cell-type-specific expression of Runx1 and Runx3 prompted the functional analyses of these transcription factors, which revealed their involvement in various processes

* Corresponding author. Fax: +81 29 853 6960.
E-mail address: tshiga@md.tsukuba.ac.jp (T. Shiga).

0012-1606/$ - see front matter © 2006 Elsevier Inc. All rights reserved.
doi:10.1016/j.ydbio.2006.12.007

of the neural development. It was shown that TrkC$^+$ DRG neurons are maintained in *Runx3*-deficient (*Runx3*$^{-/-}$) mice, but the axonal projection of proprioceptive DRG neurons to both central and peripheral targets is severely impaired (Inoue et al., 2002). Another study reported that proprioceptive DRG neurons lose their selective phenotypic markers, including TrkC, in the *Runx3*$^{-/-}$ mice (Levanon et al., 2002). Furthermore, recent studies demonstrated that Runx3 plays pivotal roles in the cell type specification of proprioceptive DRG neurons and the elaboration of their central projection to the spinal cord (Chen et al., 2006a; Kramer et al., 2006).

In contrast to Runx3, a functional analysis of Runx1 in neural development was delayed because a deficiency of Runx1 results in lethality around embryonic day (E) 11.5 due to the impaired fetal liver hematopoiesis (Okuda et al., 1996; Theriault et al., 2004, 2005; Wang et al., 1996). To overcome this limitation caused by the early embryonic lethality, Chen et al. (2006b) utilized a conditional gene targeting technique and showed that Runx1 is required for the proper cell specification and axonal projection of nociceptive DRG neurons. Although much progress has been made in the functional analysis of Runx1 in the neural development, there seems to be several discrepancies among previous studies concerning cell fate specification and axonal projections (Chen et al., 2006a,b; Kramer et al., 2006; Marmigere et al., 2006). For example, Marmigere et al. (2006) reported that Runx1 is required for the initial stage of the differentiation of TrkA$^+$ DRG neurons, whereas Chen et al. (2006b) showed that Runx1 plays a crucial role in the subsequent phenotype transition from TrkA$^+$ DRG neurons to c-ret$^+$ neurons. Marmigere et al. (2006) and Chen et al. (2006b) also reported that Runx1 is involved in the neurite outgrowth and branch formation, and proper axonal projection to the spinal cord, respectively. In the present study, to overcome the early embryonic lethality in *Runx1*$^{-/-}$ mice, we adopted a new approach by utilizing transgenic *Runx1*$^{-/-}$ mice in which liver hematopoietic cells are selectively rescued by the expression of Runx1 under the control of the *GATA-1* promoter. In these mice, *Runx1* is deficient in presumptive Runx1-expressing cells except liver hematopoietic cells. Because of the selective rescue of Runx1 in these hematopoietic cells, these mice are able to survive until late embryonic stages. We showed that Runx1 controls the cell number and cell fate specification of cutaneous DRG neurons and their axonal projections. Part of the present study has been published in abstract form (Yoshikawa et al., 2005).

Materials and methods

Genotyping and maintenance of animals

The transcription regulatory domain that directs both the primitive and definitive erythroid cell-specific expression of GATA-1 was identified previously and referred to as the *GATA-1* gene hematopoietic regulatory domain (*G1-HRD*) (Onodera et al., 1997). We exploited *G1-HRD* to rescue *Runx1* gene knockout mice from embryonic lethality by expressing the Runx1 transgene in erythroid cells specifically (Fig. 1A, Yokomizo et al., in press). Transgenic mice were generated by microinjection of DNA into fertilized BDF1 eggs using standard procedures (Wassarman and DePamphilis, 1993). Founders were screened by PCR, and verified by Southern blot analysis, using a Southern probe generated from the 4th exon sequence of the *Runx1* gene. Mice bearing the *Runx1* germ line mutant allele (Okada et al., 1998) were bred in a clean room in the Laboratory Animal Resource Center at the University of Tsukuba. *Runx1* mutant mice were genotyped as described previously (Okada et al., 1998) and a pair of primers, RUNT S1 (5′-AGCATGGTGGAGGTACTAGC-3′) and RUNT AS1 (5′-GGTCGTTGAATCTCGCTACC-3′), was used for *Runx1–Tg* detection. Phenotypes of transgenic *Runx1*$^{-/-}$ mice (*Runx1*$^{-/-}$*::Tg*) were compared with the control (*Runx1*$^{+/+}$*::Tg*) in this study. The present study was approved by the animal care committee of the University of Tsukuba.

Immunohistochemistry

For cryostat sections, E13.5 whole mouse embryos were immersed overnight at 4 °C in a fixative containing 4% paraformaldehyde in phosphate-buffered saline (PBS). Embryos at E14.5 and older were perfused transcardially with the same fixative and immersed overnight at 4 °C. The thoracic segments (Th) were dissected and immersed sequentially in 10%, 20% and 30% sucrose solutions in PBS and frozen in Tissue Tek O.C.T. compound (Sakura Finetek Japan). 10- or 12-μm transverse sections were cut and collected onto MAS-coated glass slides (Matsunami Glass Ind., Japan), and air-dried for 1 h. If needed, sections were subjected to heat induced epitope retrieval by heating to 105 °C for 5 min in Dako REAL™Target Retrieval Solution (Dako). After treatment for 30 min at room temperature (RT) with 0.3% H_2O_2 in methanol, the sections were incubated for 1 h

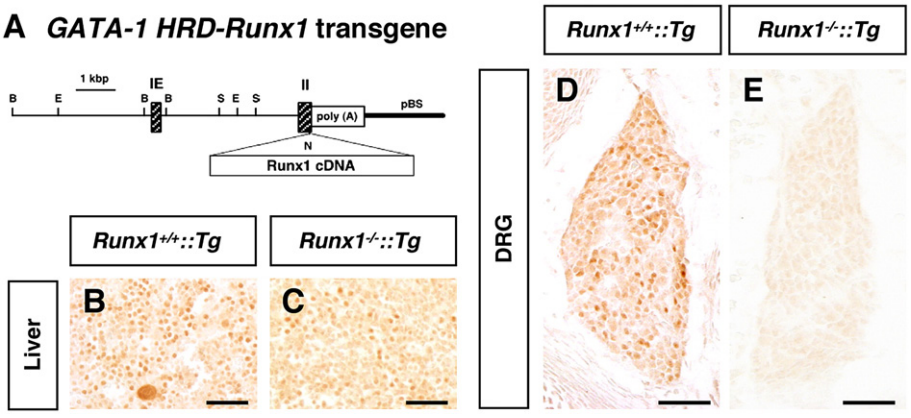

Fig. 1. Rescue of erythropoiesis in *Runx1*$^{-/-}$ mouse from early embryonic lethality with *G1-HRD–Runx1–Tg*. (A) Structure of the *G1-HRD–Runx1* transgene. This plasmid contains the 3.9-kb sequence 5′ of the IE exon, the IE exon itself, the first intron, and a part of the second exon of the mouse *GATA-1* gene in front of the Runx1 cDNA. The initiation Met codon in the second exon was replaced by a unique *Not*I site (shown as N) for subsequent cloning. Restriction enzyme sites are B, *Bam*HI; E, *Eco*RI; N, *Not*I; S, *Sac*I. (B and C) Expression of Runx1 in the liver of E14.5 *Runx1*$^{+/+}$*::Tg* (B) and *Runx1*$^{-/-}$*::Tg* (C). (D and E) Expression of Runx1 in the DRG of E14.5 *Runx1*$^{+/+}$*::Tg* (D), but expression is not observed in *Runx1*$^{-/-}$*::Tg* (E). Scale bars: 50 μm in panels B–E.

at RT in a blocking solution containing 5% normal goat serum and 0.1% Triton X-100 in PBS. For immunohistochemical analysis, the following antibodies were used: rabbit anti-RUNX1 (Sigma; 1:1000 dilution), rabbit anti-calcitonin gene-related peptide (CGRP) (Chemicon; 1:4000), goat anti-CGRP (Biogenesis; 1:4000), rabbit anti-TrkA (a gift from Dr. F. Reichardt; 1:4000), rabbit anti-TrkB (Upstate; 1:1000), goat anti-TrkC (R&D Systems; 1:2000), rabbit anti-substance P (Protos Biotech Corporation; 1:2000), rabbit anti-somatostatin (Protos Biotech Corporation; 1:2000), rabbit anti-calbindin D-28K (Swant; 1:2000), rabbit anti-VR1 (TRPV1) (Calbiochem; 1:1000), rabbit anti-VRL-1 (TRPV2) (a gift from Dr. M. Tominaga, and Calbiochem; 1:250), rabbit anti-c-ret (IBL; 1: 50), rabbit anti-parvalbumin (Swant; 1:2000), rabbit anti-peripherin (Chemicon; 1:2000), rabbit anti-active-caspase3 (Promega; 1:1000), mouse anti-BrdU (Sigma; 1:1000), mouse anti-Islet-1 (Developmental Studies Hybridoma Bank; 1:100), mouse anti-Ki67 (BD Biosciences; 1:50), rabbit anti-MAP2 (Chemicon; 1:500), and goat anti-Lmx1b (Santa Cruz Biotechnology; 1:1000). The sections were incubated overnight at 4 °C with each of the primary antibodies in the blocking solution, and then, with a biotinylated secondary antibody for 1 h at RT. The sections were incubated with the peroxidase conjugated avidin–biotin complex (Vector Laboratories; 1:100) for 30 min at RT and the positive reactions were visualized with 3, 3′-diaminobenzidine (DAB) using the ImmunoPure metal enhanced DAB substrate kit (Pierce). For triple staining, cryostat sections were incubated with anti-Islet-1 antibody, followed by the incubation with biotinylated horse anti-mouse IgG (Vector Laboratories; 1:500) and Pacific Blue conjugated Streptavidin. All the sections were then incubated with rabbit- or goat-anti-CGRP antibodies, followed by Alexa Fluor 488-labeled donkey anti-rabbit IgG or Alexa Fluor 594-labeled donkey anti-goat IgG (Invitrogen; 1:500), respectively. Subsequently, the sections were incubated either with anti-TrkB, substance P, somatostatin, calbindin D-28K, TRPV1, TRPV2, c-ret, TrkC, parvalbumin or active-caspase3, followed by Alexa Fluor 488-labeled donkey anti-rabbit IgG or Alexa Fluor 594-labeled donkey anti-goat IgG. Both *Runx1*$^{-/-}$*::Tg* and *Runx1*$^{+/+}$*::Tg* of the same littermates were processed simultaneously during the immunohistochemical processes.

Cell counting

For counts of CGRP$^+$, TrkA$^+$ and Islet-1$^+$ DRG neurons, the 10th thoracic segment (Th10)–Th12 DRGs at E17.5 were serially sectioned at 10 μm. The total number of immunoreactive neurons was counted from the level-matched thoracic DRGs of each genotype (6 DRGs from 3 embryos were examined). For cell counting of TrkB, substance P, somatostatin, calbindin D-28K, TRPV1, TRPV2, c-ret, TrkC and parvalbumin positive cells, 3–7 sections from each *Runx1*$^{+/+}$*::Tg* (14 sections from 3 embryos for each antibody) and *Runx1*$^{-/-}$*::Tg* (14 sections from 3 embryos for each antibody) were counted at identical thoracic segments. We first estimated the ratio of DRG neurons that were immunoreactive for these markers among Islet-1$^+$ DRG neurons in double stained sections, and then calculated the total number of these neurons based on the total number of Islet-1$^+$ DRG neurons in each DRG. About 1800–2500 Islet-1$^+$ DRG neurons were examined for the analysis of each marker. Furthermore, we estimated the ratio of CGRP$^+$ DRG neurons/DRG neurons immunoreactive for a given antigen (TrkA, TrkB, substance P, somatostatin, calbindin D-28K, TRPV1, TRPV2, c-ret, TrkC, and parvalbumin). In this analysis, we examined 161–1613 DRG neurons, depending on the markers (e.g., 161 parvalbumin-immunoreactive DRG neurons and 1613 TrkA-immunoreactive DRG neurons). In addition, active-caspase3-positive neurons in 8 sections from each *Runx1*$^{+/+}$*::Tg* (24 sections from 3 embryos) and each *Runx1*$^{-/-}$*::Tg* (24 sections from 3 embryos) were counted. More than 132 active-caspase3-positive neurons among more than 4111 Islet-1$^+$ DRG neurons were counted in E13.5 DRG of each *Runx1*$^{+/+}$*::Tg* and *Runx1*$^{-/-}$*::Tg*, and more than 37 active-caspase3-positive neurons among more than 6882 Islet-1$^+$ DRG neurons were counted in E17.5 DRG of each *Runx1*$^{+/+}$*::Tg* and *Runx1*$^{-/-}$*::Tg*. For cell counting, only the immunoreactive neurons containing a distinct cell nucleus were counted.

Measurement of DRG volume

Using the serial sections (10 μm thickness) containing whole Th12 DRGs at E17.5, the areas of DRG in each section were measured and the DRG volume was calculated using the AxioVision imaging software (Carl Zeiss).

BrdU labeling and detection by immunohistochemistry

At E11.5, E12.5 and E16.5, a single intraperitoneal injection of BrdU (5 mg/ml solution in PBS and 60 μg/g of body weight) was performed in pregnant mice derived from timed mating. After 24 or 48 h, the injected mice were deeply anesthetized, and embryos were removed and genotyped. Cryostat sections (10 μm thickness) of Th13 DRG were made as described above, and incubated with anti-BrdU and anti-peripherin antibodies, followed by Alexa Fluor 594-labeled donkey anti-mouse IgG and Alexa Fluor 488-labeled donkey anti-rabbit IgG (Invitrogen; 1:500). BrdU-labeled neurons in 8 sections from *Runx1*$^{+/+}$*::Tg* (24 sections from 3 embryos) and *Runx1*$^{-/-}$*::Tg* (24 sections from 3 embryos) were counted. More than 920 BrdU-labeled neurons among more than 5300 peripherin-positive DRG neurons were counted in each group.

Statistical analysis

All quantitative analyses were performed on 3 pairs of embryos from 3 independent pregnant mice. Statistical analyses were performed by ANOVA followed by post hoc analysis (Fisher's Protected Least Significant Difference Test). Differences were considered significant if the probability of error was less than 5%. All results were expressed as the mean ± SEM.

Results

Rescue of Runx1$^{-/-}$*::Tg mice by the G1-HRD–Runx1 transgene*

Runx1 knockout mice die of impaired fetal hematopoiesis by E12.5 (Okuda et al., 1996; Wang et al., 1996). This early lethality has prevented the examination of the roles of Runx1 in neural development during late embryonic and postnatal stages. In the present study, we utilized transgenic *Runx1*$^{-/-}$ mice (*Runx1*$^{-/-}$*::Tg*), in which GATA-1$^+$ hematopoietic cells are rescued by the *G1-HRD*-regulated expression of *Runx1* (Fig. 1A, Yokomizo et al., in press). At E12.5, massive hemorrhaging was observed in the head of *Runx1*$^{-/-}$ mice, whereas *Runx1*$^{-/-}$*::Tg* were viable and showed no such defects (Yokomizo et al., in press, data not shown). Immunohistochemical examination revealed that Runx1 was expressed in hematopoietic cells in the liver at E14.5 in both *Runx1*$^{+/+}$*::Tg* and *Runx1*$^{-/-}$*::Tg* (Figs. 1B, C), whereas Runx1 was expressed in DRG neurons of *Runx1*$^{+/+}$*::Tg*, but not in *Runx1*$^{-/-}$*::Tg* (Figs. 1D, E). The transgenic expression of Runx1 in hematopoietic cells allowed these animals to survive until E18.5. *Runx1*$^{+/+}$*::Tg* and *Runx1*$^{+/-}$*::Tg* were born at E19.5, but *Runx1*$^{-/-}$*::Tg* were seldom born viable. At E17.5, *Runx1*$^{-/-}$*::Tg* were often viable, but showed the hemorrhaging in the brain, subarachnoid space and subcutaneous area, probably because of the impaired blood vessel formation. Because this bleeding was mostly localized in the head and upper trunk region, but not in the lower trunk region (Supplementary Fig. 1), we examined lower thoracic regions in the present study.

Increased number of DRG neurons in Runx1$^{-/-}$*::Tg*

At E17.5, *Runx1*$^{-/-}$*::Tg* DRGs were enlarged compared with those of *Runx1*$^{+/+}$*::Tg* (Figs. 2A, B). The volume of the Th12 DRG in *Runx1*$^{-/-}$*::Tg* (0.0363 ± 0.0022 mm^3, 6 DRGs from 3 embryos) was 1.29-fold greater than that in *Runx1*$^{+/+}$*::Tg* (0.0281 ± 0.0030 mm^3, 6 DRGs from 3 embryos; $p < 0.05$) (Fig.

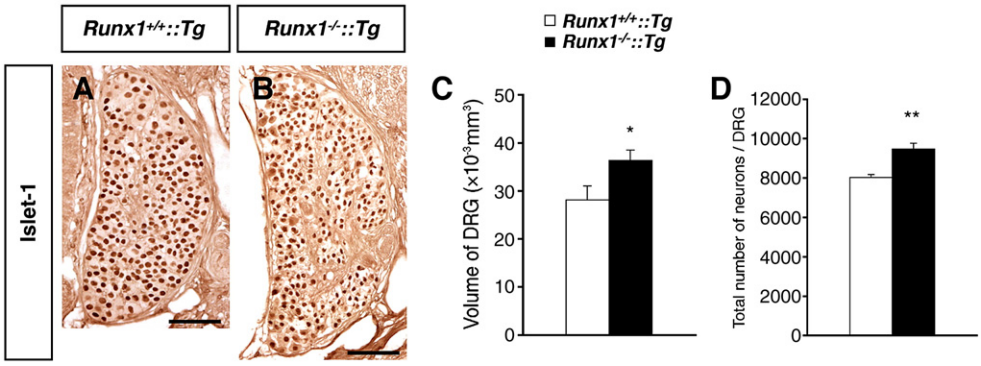

Fig. 2. The DRG neuronal number and the DRG volume are increased in E17.5 *Runx1*$^{-/-}$*::Tg*. (A and B) Photomicrographs showing the expression of Islet-1 immunoreactivity in the DRG of *Runx1*$^{+/+}$*::Tg* (A) and *Runx1*$^{-/-}$*::Tg* (B). (C and D) The volume of the DRGs (C) and the total number of Islet-1^{+} DRG neurons at the level of Th12 (D) in *Runx1*$^{+/+}$*::Tg* (open bar) and *Runx1*$^{-/-}$*::Tg* (solid bar). $n=6$ for each group. Data are shown as mean±SEM; *$p<0.05$, **$p<0.001$. Scale bars: 100 μm in panels A and B.

2C). The increased volume may reflect the number of DRG neurons, because the total number of DRG neurons also showed a 1.18-fold increase in *Runx1*$^{-/-}$*::Tg* (9477±279, 6 DRGs from 3 embryos) over that of *Runx1*$^{+/+}$*::Tg* (8028±145, 6 DRGs from 3 embryos) ($p<0.001$) (Fig. 2D).

To clarify whether the increase in the number of DRG neurons is induced by the excess proliferation of DRG progenitors and/or defective apoptosis of DRG neurons, the proliferation of DRG neuron progenitors was examined by injecting BrdU intraperitoneally into pregnant mice at E11.5 or E12.5, around the period of peak mitosis of DRG progenitors (Lawson and Biscoe, 1979). Thereafter, we examined the BrdU-labeling at E13.5, because Runx1 is not expressed in DRG until E12.5 (Chen et al., 2006b, data not shown). When we injected BrdU at E11.5 and examined the BrdU-labeled DRG neurons at E13.5, the ratio of BrdU^{+} DRG neurons per peripherin^{+} DRG neurons was increased in *Runx1*$^{-/-}$*::Tg* (17.26±0.93%) compared to that of *Runx1*$^{+/+}$*::Tg* (15.03±0.59%) ($p<0.05$) (Figs. 3A–C). In contrast, when we injected BrdU at E12.5 and examined the labeled neurons at E13.5, there was no significant difference in the ratio of BrdU^{+} DRG neurons between *Runx1*$^{+/+}$*::Tg* and *Runx1*$^{-/-}$*::Tg* (*Runx1*$^{+/+}$*::Tg*, 9.15±1.24%; *Runx1*$^{-/-}$*::Tg*, 8.25±0.54 %; $p=0.52$). Injected with BrdU at E16.5, when the mitosis of wild-type DRG neurons has ceased, virtually no BrdU^{+} neurons were observed in both *Runx1*$^{+/+}$*::Tg* and *Runx1*$^{-/-}$*::Tg* at E17.5, suggesting that the loss of Runx1 does not induce mitosis in post-mitotic DRG neurons (data not shown). Next, we double-stained E12.5 and E13.5 *Runx1*$^{+/+}$ DRGs with Runx1 antibody and Ki67 antibody to examine the presence of Runx1 in DRG progenitor cells. None of the Ki67-immunoreactive progenitors expressed Runx1 (Figs. 3D–F), confirming the results of previous reports showing that Runx1 is expressed in postmitotic DRG neurons (Chen et al., 2006b, Marmigere et al., 2006). These results suggest that the up-regulation of proliferation in *Runx1*$^{-/-}$*::Tg* DRGs may not be cell-autonomous, but mediated indirectly (e.g. by Runx1-expressing postmitotic DRG neurons or peripheral tissues). Collectively, results suggest that *Runx1* inactivation may promote the proliferation of DRG progenitor cells in a non-cell autonomous manner.

We examined the effects of Runx1-deficiency on the apoptosis of DRG neurons. At E13.5, during the peak of the programmed cell death in the mouse embryonic DRG (White et al., 1996, 1998), the percentage of caspase3-immunoreactive apoptotic cells showed a significant decrease in the DRG of *Runx1*$^{-/-}$*::Tg* (2.46±0.28%) as compared to that of *Runx1*$^{+/+}$*::Tg* (3.68±0.54%) ($p<0.05$, 24 sections from 3 embryos, for each group) (Figs. 3G–I), suggesting that Runx1 inactivation may suppress the apoptosis of DRG neurons. Unexpectedly, at E17.5, the percentage of apoptotic cells in *Runx1*$^{-/-}$*::Tg* DRG was increased by 3.1-fold over that of *Runx1*$^{+/+}$*::Tg*, although the percentage of apoptotic cells was much lower than that observed at earlier stages (*Runx1*$^{+/+}$*::Tg*, 0.60±0.13%; *Runx1*$^{-/-}$*::Tg*, 1.85±0.21%; $p<0.0001$) (Figs. 3J–L). This increase of apoptosis at late embryonic stages may be caused by mismatch between the increased number of DRG neurons and the limited amount of their targets (see below).

In summary, our results suggest that the promotion of proliferation of DRG progenitors and the suppression of apoptosis of DRG neurons by Runx1 deficiency may be responsible for the increase of DRG neurons in *Runx1*$^{-/-}$*::Tg*.

Changes of the cell fate specification in Runx1$^{-/-}$*::Tg*

In order to determine whether the increase of the neuronal number occurs in a selected population of DRG neurons in *Runx1*$^{-/-}$*::Tg*, we examined the differentiation of DRG neurons by immunohistochemistry using a variety of markers for DRG neuron subtypes. First, we counted the number of DRG neurons that were immunoreactive for TrkA and CGRP, two major markers for cutaneous neurons (Hunt et al., 1992; Ju et al., 1987; Lawson, 1992). At E17.5, an increased number of TrkA^{+} DRG neurons were observed in *Runx1*$^{-/-}$*::Tg* compared with that of *Runx1*$^{+/+}$*::Tg*. The total number of TrkA^{+} neurons in the Th11 DRG was increased by 1.43-fold in *Runx1*$^{-/-}$*::Tg* (6608±224, 6 DRGs from 3 embryos) compared with that of *Runx1*$^{+/+}$*::Tg* (4634±116, 6 DRGs from 3 embryos) ($p<0.0001$) (Figs. 4A, B, E). Concomitantly, the total number of CGRP^{+} neurons in the Th10 DRG was greatly increased by

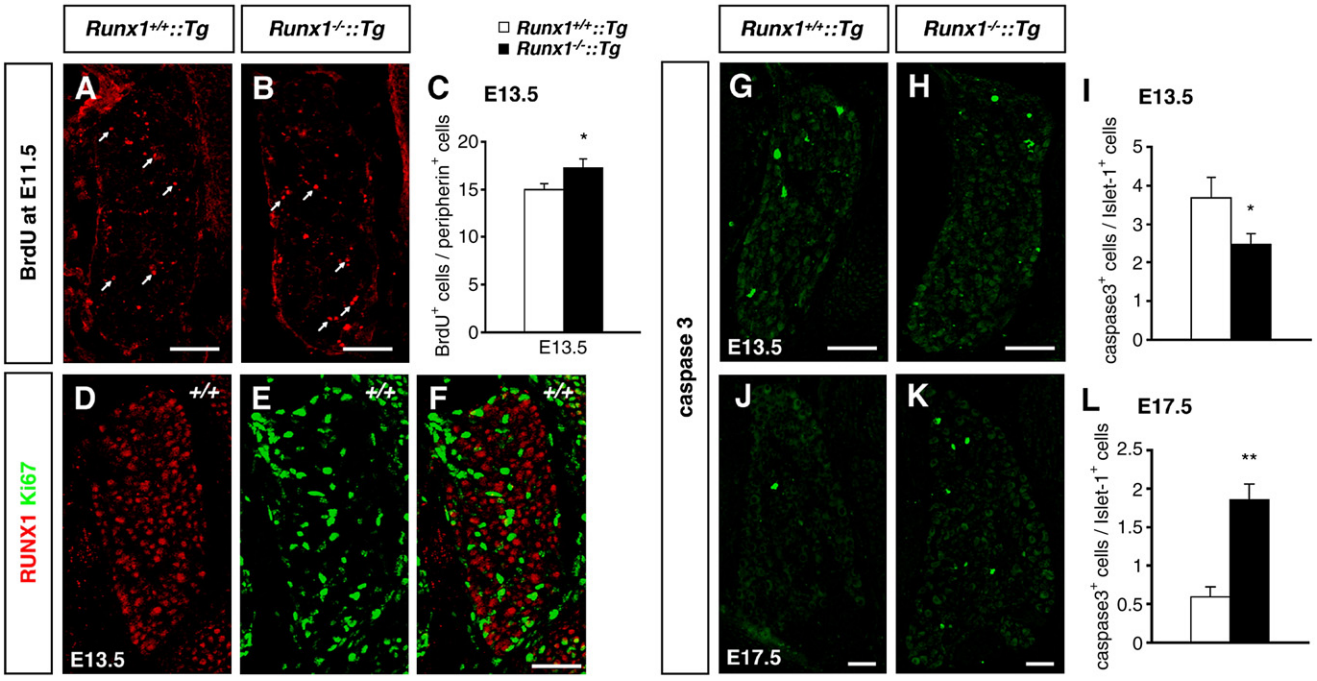

Fig. 3. DRG increased proliferative activity, but decreased apoptosis in E13.5 *Runx1*$^{-/-}$*::Tg*. (A and B) BrdU$^+$ neurons in the DRG of *Runx1*$^{+/+}$*::Tg* (A) and *Runx1*$^{-/-}$*::Tg* (B) which received BrdU at E11.5 and were sacrificed at E13.5. Arrows indicated examples of BrdU$^+$ neurons. (C) Quantitative analysis of the number of BrdU$^+$ neurons in E13.5 *Runx1*$^{+/+}$*::Tg* and *Runx1*$^{-/-}$*::Tg* DRG. (D–F) Detection of Runx1$^+$ (red)/Ki67$^+$ (green) in the DRG of E13.5 *Runx1*$^{+/+}$*::Tg*. (G and H) Immunohistochemical detection of caspase3 in E13.5 *Runx1*$^{+/+}$*::Tg* (G) and *Runx1*$^{-/-}$*::Tg* (H) DRG neurons. (I) At E13.5, the percentage of caspase3$^+$ neurons showed a slight decrease in cell death in the DRG of *Runx1*$^{-/-}$*::Tg*. (J and K) Caspase3 expression in E17.5 *Runx1*$^{+/+}$*::Tg* (J) and *Runx1*$^{-/-}$*::Tg* (K) DRG neurons. (L) At E17.5, the percentage of cell death in the DRG of *Runx1*$^{-/-}$*::Tg* was increased. Data are shown as mean±SEM; *$p<0.05$, **$p<0.001$. Scale bars: 50 μm in panels A, B, D, E, F, G, H; 100 μm in panels J and K.

2.74-fold in *Runx1*$^{-/-}$*::Tg* (2454±50) compared with that of *Runx1*$^{+/+}$*::Tg* (894±40, 6 DRGs from 3 embryos for each group) ($p<0.0001$) (Figs. 4C–E). The increase of both TrkA$^+$ DRG neurons and CGRP$^+$ DRG neurons was also observed at E16.5 (TrkA$^+$ neurons: 2919 in *Runx1*$^{+/+}$*::Tg* and 4478 in *Runx1*$^{-/-}$*::Tg*; CGRP$^+$ neurons: 678 in *Runx1*$^{+/+}$*::Tg* and 1431 in *Runx1*$^{-/-}$*::Tg*, 2 DRGs from 1 embryo for each group).

In order to examine in more detail the effects of *Runx1* deficiency in the cell fate specification, E17.5 DRG neurons at the level of Th6–8 were triple-stained with antibodies against neurotrophin receptors (TrkB, TrkC, c-ret), neuropeptides (substance P, somatostatin), calcium binding proteins (calbindin D-28K, parvalbumin), and TRP channels (TRPV1, TRPV2) in combination with anti-Islet-1 and anti-CGRP antibodies. TrkC and parvalbumin are markers for proprioceptive DRG neurons, and were used for comparison with cutaneous DRG markers. We first estimated the ratio of DRG neurons that were immunoreactive for these markers among Islet-1$^+$ DRG neurons in selected sections (14 sections from 3 embryos), and then calculated the total number of these neurons based on the total number of Islet-1$^+$ DRG neurons in each DRG (Fig. 4F). Somatostatin$^+$ DRG neurons were increased by 1.81-fold ($p<0.005$) in *Runx1*$^{-/-}$*::Tg* (1446±186) compared with that of *Runx1*$^{+/+}$*::Tg* (799±94). Among the somatostatin$^+$ DRG neurons, the number of neurons expressing a low level of somatostatin was increased from 666± 82 (*Runx1*$^{+/+}$*::Tg*) to 1297±178 (*Runx1*$^{-/-}$*::Tg*) ($p<0.005$). In contrast, c-ret-immunoreactive neurons were greatly decreased by 0.49-fold ($p<0.005$) in *Runx1*$^{-/-}$*::Tg* (967±102) compared with that of *Runx1*$^{+/+}$*::Tg* (1962±154). Unexpectedly, TrkC$^+$ DRG neurons were increased by 1.48-fold (*Runx1*$^{+/+}$*::Tg*, 1023±101; *Runx1*$^{-/-}$*::Tg*, 1509±95; $p<0.005$). No significant differences were observed in the number of DRG neurons immunoreactive for TrkB, substance P, calbindin D-28K, TRPV1, TRPV2, and parvalbumin (Fig. 4F). The number of TRPV1$^+$ DRG neurons was similar between *Runx1*$^{+/+}$*::Tg* (1797±206) and *Runx1*$^{-/-}$*::Tg* (1672±191), but the number of DRG neurons expressing a high level of TRPV1 was decreased from 1114± 133 (*Runx1*$^{+/+}$*::Tg*) to 456±57 (*Runx1*$^{-/-}$*::Tg*) ($p<0.001$). These results suggest that the Runx1 deficiency affected the cell fate of DRG neurons characterized by the expression of specific biochemical markers.

Ectopic expression of CGRP in Runx1$^{-/-}$*::Tg*

As described above, the total number of CGRP$^+$ DRG neurons was greatly increased in E17.5 *Runx1*$^{-/-}$*::Tg*. Then we examined the subtypes of DRG neurons that contributed to this increase of CGRP expression. We stained DRG neurons using antibodies against TrkA, TrkB, TrkC, substance P, somatostatin, calbindin D-28K, parvalbumin, TRPV1, TRPV2 or c-ret in combination with CGRP antibody (Fig. 5). Then, we estimated the ratio of CGRP$^+$ DRG neurons/DRG neurons

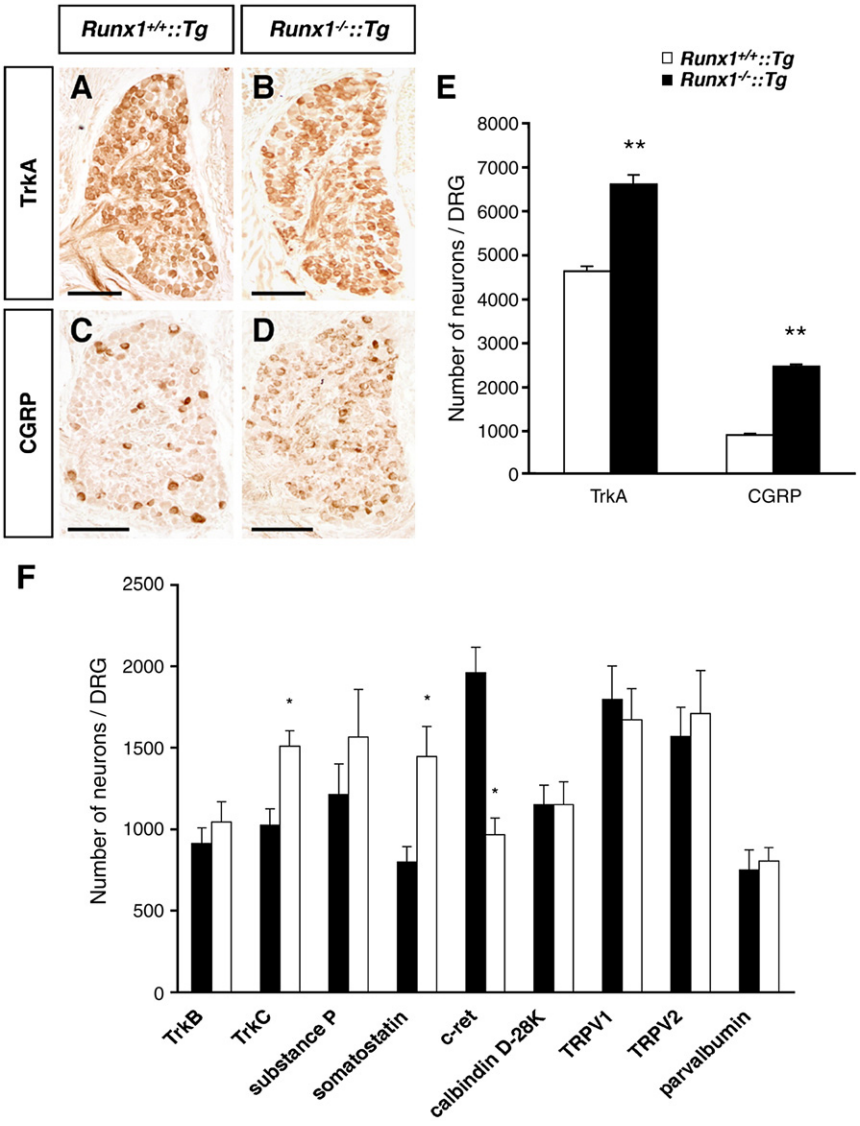

Fig. 4. Cell-type-specific changes in the number of DRG neurons in *Runx1*$^{-/-}$*::Tg* at E17.5. (A–D) The expression of TrkA (A, B) and CGRP (C, D) in *Runx1*$^{+/+}$*::Tg* (A, C) and *Runx1*$^{-/-}$*::Tg* (B, D). (E) Quantitative analysis of the total number of CGRP^{+} DRG neurons at Th10 and TrkA^{+} DRG neurons at Th11. $n=6$ for each group. (F) The total number of DRG neurons that express the various neuronal markers. Somatostatin^{+} and TrkC^{+} DRG neurons are increased in *Runx1*$^{-/-}$*::Tg*, whereas c-ret^{+} neurons are decreased in *Runx1*$^{-/-}$*::Tg*. Data are shown as mean ± SEM; *$p<0.005$, **$p<0.0001$. Scale bars: 100 μm in panels A–D.

immunoreactive for a given antigen. CGRP expression was differentially regulated among the DRG neuron subtypes in wild type mice. For example, more than 60% of substance P^{+} neurons expressed CGRP, while less than 20% of TrkC^{+} neurons expressed this neuropeptide. In *Runx1*$^{-/-}$*::Tg*, the ratio of CGRP-expressing neurons increased in all subtypes examined. For example, 18% of TrkA^{+} DRG neurons co-expressed CGRP in *Runx1*$^{+/+}$*::Tg*, whereas 76% of TrkA^{+} DRG neurons co-expressed CGRP in *Runx1*$^{-/-}$*::Tg*. The higher rate of co-expression with CGRP and TrkA in *Runx1*$^{-/-}$*::Tg* compared with the results in Fig. 4E may be due to a higher sensitivity of the immunofluorescence method over that of the DAB method. These results suggest that CGRP expression may be suppressed directly or indirectly by Runx1 in DRG neurons that express TrkA, TrkB, TrkC, substance P, somatostatin, calbindin D-28K, parvalbumin, TRPV1, TRPV2 or c-ret.

Changes in the central and peripheral projection patterns of DRG neurons in Runx1$^{-/-}$*::Tg*

We examined the axonal projections of DRG neurons toward central and peripheral targets. In *Runx1*$^{+/+}$*::Tg*, CGRP^{+} neurons appeared in the DRG by E14.5 and increased thereafter (Figs. 6A, C). CGRP^{+} DRG axons entered the spinal cord by E15.5, and penetrated the dorsal horn by E16.5 (Figs. 6E, G). In accordance with the increase of the CGRP^{+} DRG neurons (Figs. 4 and 6B, D), a more dense projection of CGRP^{+} axons was detected at E15.5 in *Runx1*$^{-/-}$*::Tg* compared with that *Runx1*$^{+/+}$*::Tg* (Figs. 6E, F). The increase of CGRP^{+} axons was apparent by E17.5, as more CGRP^{+} axons were distributed in a wider range of laminae of the dorsal horn in *Runx1*$^{-/-}$*::Tg* (Figs. 6I, J). CGRP was co-localized in most of the TrkA^{+} axons in *Runx1*$^{-/-}$*::Tg*, while CGRP^{+} DRG

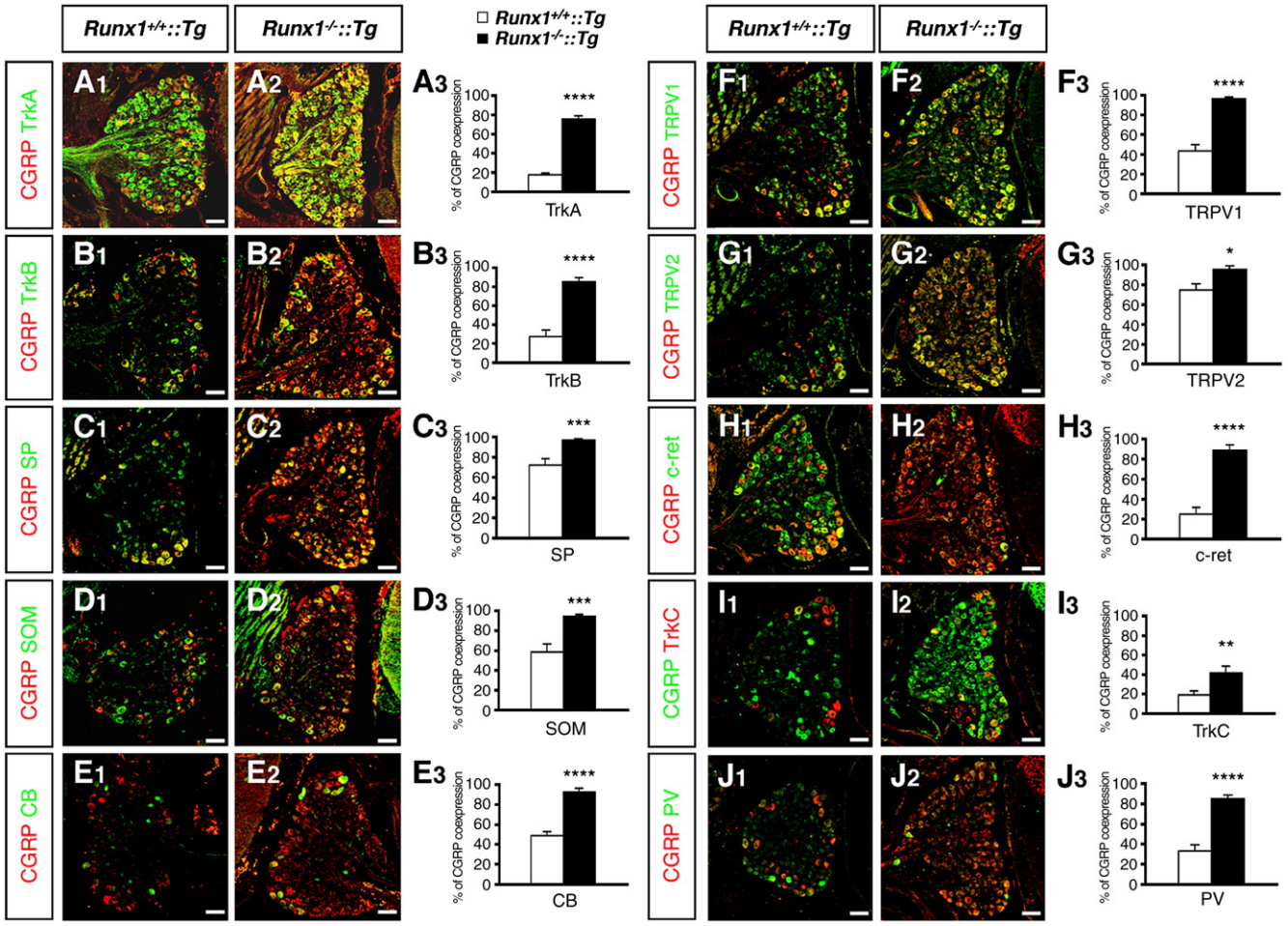

Fig. 5. Increase of co-expression with CGRP in *Runx1*$^{-/-}$*::Tg* DRG at E17.5. (A1–J1, A2–J2) Double staining of TrkA (A1, A2), TrkB (B1, B2), substance P (C1, C2), somatostatin (D1, D2), calbindin D-28K (E1, E2), TRPV1 (F1, F2), TRPV2 (G1, G2), c-ret (H1, H2), TrkC (I1, I2) and parvalbumin (J1, J2) in combination with CGRP in the DRG of *Runx1*$^{+/+}$*::Tg* (A1, B1, C1, D1, E1, F1, G1, H1, I1, J1) and *Runx1*$^{-/-}$*::Tg* (A2, B2, C2, D2, E2, F2, G2, H2, I2, J2) DRG neuron at E17.5. (A3–J3) The ratio of CGRP^{+} DRG neurons/DRG neurons immunoreactive for a given antigen in *Runx1*$^{-/-}$*::Tg* DRG are increased compared with *Runx1*$^{+/+}$*::Tg* at E17.5 (A3, B3, C3, D3, E3, F3, G3, H3, I3, J3). SP: substance P, SOM: somatostatin, CB: calbindin D-28K, PV: parvalbumin. Data are shown as mean±SEM; *$p<0.05$, **$p<0.01$, ***$p<0.001$, ****$p<0.0001$. Scale bars: 50 μm in panels A1–J1 and A2–J2.

axons were predominantly distributed in the superficial dorsal horn in *Runx1*$^{+/+}$*::Tg* (Figs. 6K, L). Double staining with MAP2 or Lmx1b antibodies and CGRP antibody revealed that CGRP^{+} DRG axons were distributed in laminae I and II in *Runx1*$^{-/-}$*::Tg*, whereas these axons were localized in the superficial layer in *Runx1*$^{+/+}$*::Tg* (Figs. 6O–R) (Ding et al., 2004). Similar ventral expansion of axonal projections was observed in somatostatin^{+} axons in *Runx1*$^{-/-}$*::Tg* (Figs. 6M, N). In addition, MAP2 staining showed that the laminar pattern of dorsal horn neurons was not affected by Runx1-deficiency (Figs. 6O, P).

The expression of TrkA and CGRP was also up-regulated in peripheral DRG axons of *Runx1*-deficient animals. In the dorsal skin of *Runx1*$^{+/+}$*::Tg* at E17.5, TrkA^{+} DRG axons and CGRP^{+} axons were detected in the dermis and the base of the epidermis as thick fiber bundles (Fig. 7). In *Runx1*$^{-/-}$*::Tg*, TrkA^{+} DRG axons were increased, especially in the dermis, and most of these axons co-expressed CGRP (Fig. 7). During the stages examined, neither substance P^{+} nor somatostatin^{+} axons were observed in the dorsal skin of *Runx1*$^{+/+}$*::Tg* or *Runx1*$^{-/-}$*::Tg*.

Discussion

Rescue of Runx1 expression in hematopoietic cells, but not in DRG neurons

Runx1$^{-/-}$ embryos die by E12.5 because of impaired fetal hematopoiesis in the liver (Okuda et al., 1996; Wang et al., 1996). In order to examine the role of Runx1 in neural development, Chen et al. (2006b) generated a conditional Runx1 knockout mice by crossing mice that carry a lox P-based conditional Runx1 allele and Wnt1-Cre mice that direct Cre expression in premigratory neural crest cells, including progenitors of DRG neurons. In these mice, Runx1 function is selectively impaired in cells of neural crest origin including DRG neurons. In contrast, we took a different approach to overcome the early embryonic lethality in *Runx1*$^{-/-}$ embryos.

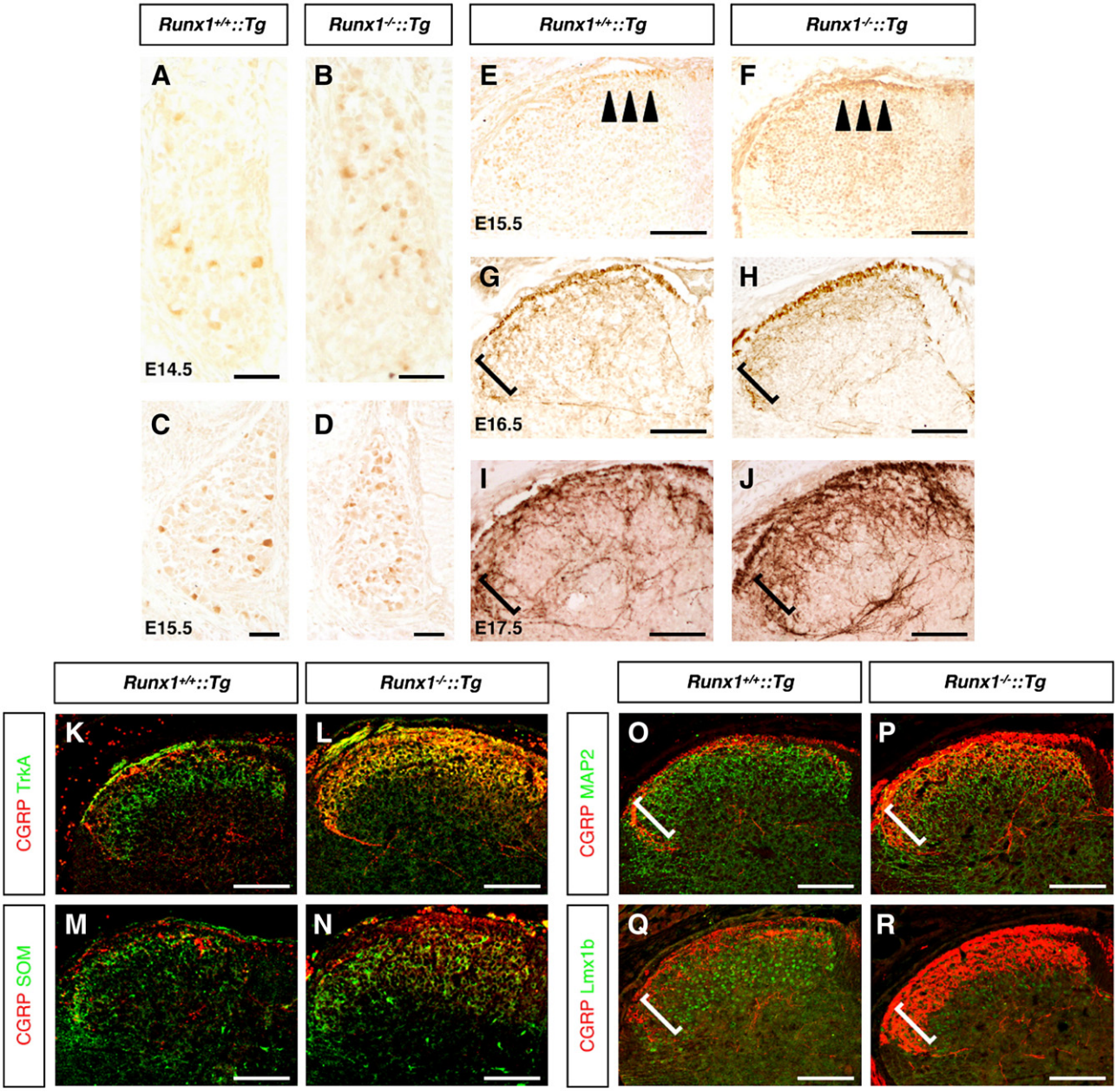

Fig. 6. CGRP expression in the DRG and the dorsal horn. (A–D) CGRP$^+$ DRG neurons in *Runx1*$^{+/+}$*::Tg* (A, C) and *Runx1*$^{-/-}$*::Tg* (B, D) at E14.5 (A, B) and E15.5 (C, D). (E and F) CGRP$^+$ axons (arrowheads) in the dorsal funiculus of E15.5 *Runx1*$^{+/+}$*::Tg* (E) and *Runx1*$^{-/-}$*::Tg* (F). (G–J) CGRP$^+$ axons in the superficial dorsal horn of *Runx1*$^{+/+}$*::Tg* (G, I) and *Runx1*$^{-/-}$*::Tg* (H, J) at E16.5 (G, H) and E17.5 (I, J). (K–R) Double staining of CGRP and TrkA (K, L), somatostatin (M, N), MAP2 (O, P) and Lmx1b (Q, R) in *Runx1*$^{+/+}$*::Tg* (K, M, O, Q) and *Runx1*$^{-/-}$*::Tg* (L, N, P, R) at E17.5. Bracket in panels O–R shows laminae I–II. Scale bars: 50 μm in panels A–D; 100 μm in panels E–R.

We utilized transgenic *Runx1*$^{-/-}$ mice, in which GATA-1$^+$ hematopoietic cells are rescued by *G1-HRD*-regulated expression of Runx1. Since GATA-1 is expressed only in a limited number of cell types such as hematopoietic cells and Sertoli cells in the testis (Burch, 2005), hematopoietic cells in the liver were rescued in their expression of Runx1, whereas Runx1 expression remained deleted in most other cells such as sensory ganglia and epidermal appendages (Levanon et al., 2001; Simeone et al., 1995). These mice survive until late embryonic stages, and thus, we were able to analyze the roles of Runx1 in the development of DRGs.

Regulation of neuronal number by Runx1

The present study demonstrated that the total number of DRG neurons was increased in *Runx1*$^{-/-}$*::Tg*. To elucidate the mechanisms underlying this increase, we investigated the effects of cell proliferation and apoptosis. The peak of the mitosis of DRG progenitors occurs around E11.5 (Lawson and Biscoe, 1979). When we applied BrdU at E11.5 and examined the DRG at E13.5, the ratio of BrdU$^+$ DRG neurons was significantly increased in *Runx1*$^{-/-}$*::Tg*, suggesting that Runx1 may negatively regulate the proliferation of DRG progenitor

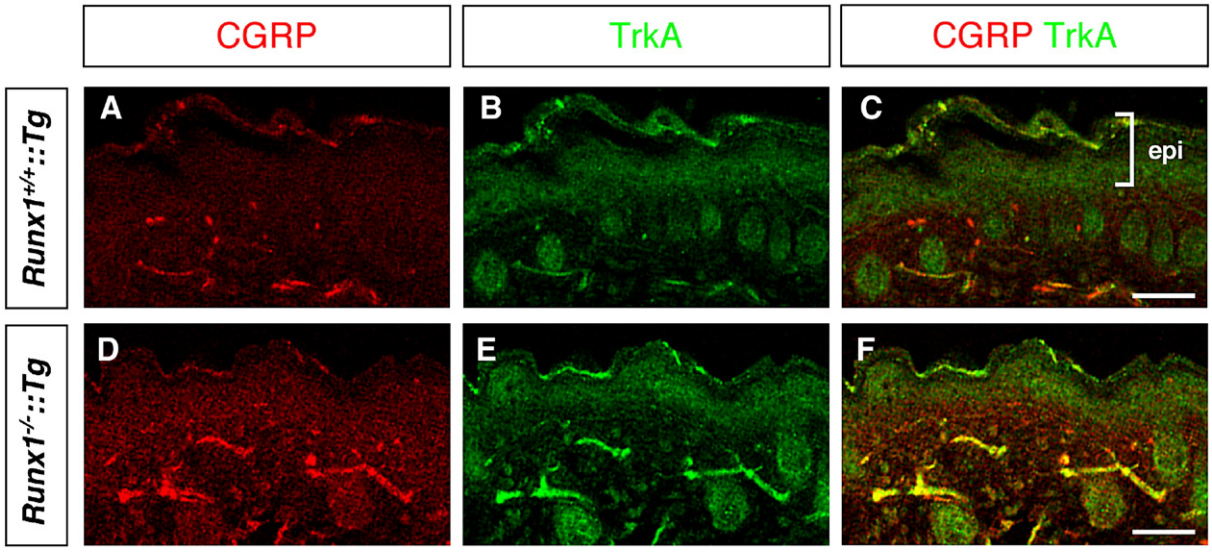

Fig. 7. Both CGRP$^+$ axons and TrkA$^+$ axons are increased in the dermis and the base of epidermis (epi) of *Runx1*$^{-/-}$*::Tg*. Double staining of CGRP$^+$ axons (A, D) and TrkA$^+$ axons (B, E) in the dorsal skin of *Runx1*$^{+/+}$*::Tg* (A–C) and *Runx1*$^{-/-}$*::Tg* (D–F) at E17.5. Scale bars: 50 μm in panels C and F.

cells. Previous studies reported that *Runx1* mRNA is detected in presumptive postmitotic DRG neurons at E10.5 (Marmigere et al., 2006) and that Runx1 is first expressed in TrkA$^+$ postmitotic DRG neurons at E12.5 (Chen et al., 2006a,b). Our results also showed that Runx1 was not expressed in proliferating DRG progenitors. These findings suggest that the effects of Runx1 deficiency on the proliferation of DRG progenitors may not be cell-autonomous, but may be mediated indirectly through other Runx1-expressing cells. Another possibility may be considered that Runx1 acts as a differentiation factor for DRG neurons to induce the cell differentiation of the DRG progenitors. However, this possibility is unlikely because at least TrkA$^+$ DRG neurons differentiate in *Runx1*$^{-/-}$ mice from the early embryonic stages (unpublished observation, and Chen et al., 2006b).

In addition to the increased proliferative activity, a decrease of apoptosis during the peak apoptotic stages (White et al., 1996, 1998) may also contribute to the increase in the total number of DRG neurons in the *Runx1*$^{-/-}$*::Tg*. The apoptosis that occurred in the mutant DRG at late embryonic stages (E17.5) may be caused by the mismatch between the increased number of DRG neurons and their targets (Oppenheim, 1991). The present study showed the increase of both the total number of DRG neurons and the axonal projection of TrkA$^+$ and CGRP$^+$ axons in the *Runx1*$^{-/-}$*::Tg*. No apparent changes in the targets in skin and spinal cord may limit trophic factors to support the increased DRG neurons. Although the increased apoptosis may be caused by the Runx1-deficiency, we cannot exclude the possibility that the apoptosis may be non-specific, because hemorrhage was often observed at E17.5.

The total number of neurons together with TrkA$^+$ neurons has been reported to be decreased in the *Runx1*$^{-/-}$ trigeminal ganglia (Theriault et al., 2004). Furthermore, in these mutant ganglia, TUNEL-positive apoptotic cells were increased with no changes in the mitotic activity, suggesting that changing the activity of apoptosis but not proliferation induces a decrease of trigeminal ganglion neurons (Theriault et al., 2004). Together, these results suggest that *Runx1* plays different roles in the regulation of cell number (proliferation and apoptosis) between DRGs and trigeminal ganglia. In addition, *Runx3*$^{-/-}$ mice showed a decreased number of DRG neurons as compared with *Runx3*$^{+/+}$ mice (Inoue et al., 2002; Shiga et al., unpublished observation). Although mechanisms remain to be examined, these results suggest a different role of Runx1 and Runx3 in the regulation of DRG neuronal number.

Role of Runx1 in the differentiation of cutaneous DRG neurons

Neural crest cells begin to migrate from the neural tube at E9 in mice (Serbedzija et al., 1990). In the course of DRG formation, cutaneous neurons begin to express TrkA at the initial stages of the development (Huang and Reichardt, 2001), and, shortly thereafter, most of these TrkA$^+$ neurons express Runx1 (Chen et al., 2006b; Marmigere et al., 2006). Subsequently, during late embryonic and postnatal stages, some TrkA$^+$ DRG neurons suppress TrkA expression and induce c-ret (TrkA$^-$/c-ret$^+$ neurons), while other TrkA$^+$ DRG neurons retain TrkA expression and induce CGRP (TrkA$^+$/CGRP$^+$/c-ret$^-$ neurons) (Molliver et al., 1997). Thus, the switch for neurotrophin dependence occurs from nerve growth factor (NGF)-dependent TrkA$^+$ neurons to glial-cell-line-derived neurotrophic factor (GDNF)-dependent c-ret$^+$ neurons. Recent loss-of function and gain-of-function studies have elucidated the significance of Runx1 in the cell fate specification of these TrkA$^+$ DRG neurons (Chen et al., 2006b; Kramer et al., 2006; Marmigere et al., 2006). Marmigere et al. (2006) reported that the loss of Runt activity in chick embryos depletes TrkA expression in DRG neurons, leading to the neuronal death, while the ectopic expression of Runx1 specifically induces the expression of TrkA, but not TrkB nor TrkC, showing that Runx1 is required for the initial establishment of TrkA$^+$ DRG neurons. In contrast, Chen et al. (2006b) demonstrated that

during this phenotype transition, the persistent expression of Runx1 marks DRG neurons that change from the initial TrkA$^+$ to TrkA$^-$/c-ret$^+$ phenotype, while the loss of Runx1 expression marks DRG neurons with the TrkA$^+$/CGRP$^+$/c-ret$^-$ phenotype, suggesting that Runx1 is involved in this phenotype transition. This possibility was verified by the experimental analyses showing that Runx1 function is essential for the transition from TrkA$^+$ to TrkA$^-$/c-ret$^+$ phenotype in a subset of cutaneous DRG neurons and that Runx1 expression suppresses CGRP expression (Chen et al., 2006b; Kramer et al., 2006). The current study using a different transgenic strategy showed that TrkA$^+$ DRG neurons appeared in *Runx1*$^{-/-}$ mice and that *Runx1*-deficiency increased the total number of TrkA$^+$ and CGRP$^+$ DRG neurons accompanied with a decrease in c-ret$^+$ DRG neurons at late embryonic stages. Thus, our results support the findings of the latter studies that Runx1 may induce c-ret expression and suppress CGRP expression. The increase of TrkA$^+$ DRG neurons observed in the present study may be due to an impaired switch from the TrkA$^+$ to TrkA$^-$/c-ret$^+$ phenotype. Otherwise, Runx1 may regulate negatively the number of TrkA$^+$ DRG neurons by way of controlling the proliferation and apoptosis, as discussed above. Taken together, Runx1 is likely to play essential roles in the cell specification of nociceptive DRG neurons by inducing c-ret expression with concomitant suppression of TrkA and CGRP expression.

CGRP expression in DRG neurons has been reported to be regulated by various factors including NGF, activin, BMP2, BMP4, BMP6, and interleukin-1 beta, some of which are produced by keratinocytes in the skin (Ai et al., 1999; Hall et al., 2001; Hou et al., 2003; Moqrich et al., 2004; Patel et al., 2000; Ritter et al., 1991; Watson et al., 1995) Therefore, several mechanisms may underlie the increase of CGRP$^+$ DRG neurons observed in *Runx1*$^{-/-}$*::Tg* in the present study. One possible mechanism is that Runx1 directly suppresses the CGRP gene expression and the Runx1-deficiency de-represses CGRP expression. The other possibility is an indirect mechanism by which Runx1 may control the responsiveness for NGF, activin, BMP2, BMP4, BMP6 and other factors. Finally, Runx1 expressing keratinocytes may be influenced by the Runx1-deficiency to up-regulate CGRP$^+$ DRG neurons through the various factors described above (Levanon et al., 2001; Lian et al., 2003).

The expression of other neuropeptides is also controlled by Runx1 in the nociceptive DRG neurons. Chen et al. (2006b) reported that the Runx1-deficiency induced a modest increase of substance P$^+$ DRG neurons in contrast to the marked increase of CGRP$^+$ neurons, although the ectopic expression of Runx1 did not result in changes in the expression of substance P (Kramer et al., 2006). The present study showed that somatostatin$^+$ DRG neurons were increased, whereas SP$^+$ neurons did not show a significant increase. Therefore, in addition to CGRP, the expression of neuropeptides including somatostatin may be down-regulated by Runx1.

Furthermore, the present study showed that the number of DRG neurons expressing a high level of TRPV1 was decreased in *Runx1*$^{-/-}$*::Tg*, supporting results of the previous study (Chen et al., 2006b). Chen et al. (2006b) suggested that Runx1 may regulate the expression of a variety of proteins critical for nociceptive function, which was accompanied by the behavioral defects in nociception. In *Runx1*$^{-/-}$ mice, many genes that are expressed in c-ret$^+$/IB4$^+$ neurons, including TRP class ion channels and ATP-gated P2X3 channels, are completely eliminated or greatly reduced, whereas others that are preferentially expressed in TrkA$^+$ neurons, including DTASIC and MOR, are expanded. It remained to be elucidated the relationships between TrkA expression and the expression of other proteins specific for nociceptive DRG neurons, because the expression of the Trk receptor can specify phenotype of DRG neurons (Moqrich et al., 2004).

The present study showed that TrkC$^+$ DRG neurons were affected by Runx1-deficiency. The TrkC$^+$ neurons were increased in *Runx1*$^{-/-}$*::Tg* (Fig. 4F), and CGRP expression in TrkC$^+$ neurons and parvalbumin$^+$ neurons was also increased (Fig. 5). In addition to these changes, axons of TrkC$^+$ neurons and parvalbumin$^+$ neurons were more fasciculated and undulating in the spinal cord (unpublished observation). Although Runx1 is not expressed in the TrkC$^+$ DRG neurons (Chen et al., 2006b; Marmigere et al., 2006), subpopulation of TrkC$^+$ DRG neurons innervate mechanoreceptors (Kirstein and Farinas, 2002). Therefore, these mechanoreceptive TrkC$^+$ DRG neurons may be indirectly affected by Runx1-expressing tissues.

Regulation of neurite outgrowth and axonal projection by Runx1

In addition to cell fate specification, Runx1 is involved in the neurite outgrowth and axonal projection of DRG neurons (Marmigere et al., 2006; Chen et al., 2006b). Marmigere et al. (2006) have reported that the overexpression of Runx1 in combination with Neurogenin-2 in neural crest stem cells promotes neurite outgrowth and branching formation in vitro. In *Runx1*$^{-/-}$ mice, DRG axons enter the spinal cord as in the wild type mice, but a subset of DRG neurons fail to project to the specific lamina in the dorsal horn (Chen et al., 2006b). In wild-type adult mice, TrkA$^+$ DRG axons project predominantly to lamina I and the outer layer of lamina II (IIo) in the dorsal horn, whereas Ret$^+$ axons, which can also be labeled by the lectin IB4, project predominantly to the inner layer of lamina II (IIi) (Molliver et al., 1997; Snider and McMahon, 1998). In the present study of late embryonic stages, we observed that, in the *Runx1*$^{-/-}$*::Tg*, axonal projections of CGRP$^+$ DRG neurons, which normally project to I/IIo, expanded to IIi, as well as I/IIo. However, we could not analyze the axonal projection of IB4$^+$ axons because IB4 binding appears in DRG axons after birth. Most of these CGRP$^+$ axons co-expressed TrkA$^+$, consistent with the increase of CGRP$^+$ DRG neurons co-expressing TrkA. This was also the case in the peripheral projection where increased CGRP$^+$ axons in the skin co-expressed TrkA. Chen et al. (2006b) showed that the loss of Runx1 function changes the targeting of the IB4$^+$ axonal projection from lamina IIi to the superficial laminae I/IIo. In these *Runx1*$^{-/-}$ mice, CGRP$^+$ axons remain predominantly in laminae I/IIo, as in the wild

type. Thus, the projection of $IB4^+$ axons shifted dorsally from IIi to I/IIo without changes in the $CGRP^+$ axonal projections. Therefore, there seems to be a discrepancy concerning the projection of $CGRP^+$ axons to the dorsal horn between the present and previous study (Chen et al., 2006b). It is likely that this discrepancy is due to the ages of the mice. It would be interesting to examine the ventrally expanded projection of $CGRP^+$ axons during postnatal stages, to determine whether mis-routed axonal projections are retained or eliminated.

Acknowledgments

The authors thank Drs. M. Tominaga, and F. Reichard for providing the antibodies against TRPV2 and TrkA, respectively. This study was supported by a grant-in-aid for scientific research from the 21st Century COE Program from the Ministry of Education, Culture, Sports, Science and Technology (MEXT) of Japan.

Appendix A. Supplementary data

Supplementary data associated with this article can be found, in the online version, at doi:10.1016/j.ydbio.2006.12.007.

References

Ai, X., Cappuzzello, J., Hall, A.K., 1999. Activin and bone morphogenetic proteins induce calcitonin gene-related peptide in embryonic sensory neurons *in vitro*. Mol. Cell. Neurosci. 14, 506–518.

Burch, J.B., 2005. Regulation of *GATA* gene expression during vertebrate development. Semin. Cell Dev. Biol. 16, 71–81.

Chen, A.I., de Nooij, J.C., Jessell, T.M., 2006a. Graded activity of transcription factor Runx3 specifies the laminar termination pattern of sensory axons in the developing spinal cord. Neuron 49, 395–408.

Chen, C.L., Broom, D.C., Liu, Y., de Nooij, J.C., Li, Z., Cen, C., Samad, O.A., Jessell, T.M., Woolf, C.J., Ma, Q., 2006b. Runx1 determines nociceptive sensory neuron phenotype and is required for thermal and neuropathic pain. Neuron 49, 365–377.

Coffman, J.A., 2003. Runx transcription factors and the developmental balance between cell proliferation and differentiation. Cell Biol. Int. 27, 315–324.

De Brujin, M.F., Speck, N.A., 2004. Core-binding factors in hematopoiesis and immune function. Oncogene 23, 4238–4248.

Ding, Y.Q., Yin, J., Kania, A., Zhao, Z.Q., Johnson, R.L., Chen, Z.F., 2004. Lmx1b controls the differentiation and migration of the superficial dorsal horn neurons of the spinal cord. Development 131, 3693–3703.

Dormand, E.L., Brand, A.H., 1998. Runt determines cell fates in the *Drosophila* embryonic CNS. Development 125, 1659–1667.

Duffy, J.B., Kania, M.A., Gergen, J.P., 1991. Expression and function of the *Drosophila* gene *runt* in early stages of neural development. Development 113, 1223–1230.

Hall, A.K., Dinsio, K.J., Cappuzzello, J., 2001. Skin cell induction of calcitonin gene-related peptide in embryonic sensory neurons in vitro involves activin. Dev. Biol. 229, 263–270.

Hou, L., Li, W., Wang, X., 2003. Mechanism of interleukin-1 beta-induced calcitonin gene-related peptide production from dorsal root ganglion neurons of neonatal rats. J. Neurosci. Res. 73, 188–197.

Huang, E.J., Reichardt, L.F., 2001. Neurotrophins: roles in neuronal development and function. Annu. Rev. Neurosci. 24, 677–736.

Hunt, S.P., Mantyh, P.W., Priestley, J.V., 1992. The organization of biochemically characterized sensory neurons. In: Scott, S.A. (Ed.), Sensory Neurons. Oxford Univ. Press, New York, pp. 60–76.

Inoue, K., Ozaki, S., Shiga, T., Ito, K., Masuda, T., Okado, N., Iseda, T., Kawaguchi, S., Ogawa, M., Bae, S.C., Yamashita, N., Itohara, S., Kudo, N., Ito, Y., 2002. Runx3 controls the axonal projection of proprioceptive dorsal root ganglion neurons. Nat. Neurosci. 5, 946–954.

Ito, Y., 2004. Oncogenic potential of the *RUNX* gene family: overview. Oncogene 23, 4198–4208.

Ju, G., Hokfelt, T., Brodin, E., Fahrenkrug, J., Fischer, J.A., Frey, P., Elde, R.P., Brown, J.C., 1987. Primary sensory neurons of the rat showing calcitonin gene-related peptide immunoreactivity and their relation to substance P-, somatostatin-, galanin-, vasoactive intestinal polypeptide- and cholecystokinin-immunoreactive ganglion cells. Cell Tissue Res. 247, 417–431.

Kirstein, M., Farinas, I., 2002. Sensing life: regulation of sensory neuron survival by neurotrophins. Cell. Mol. Life Sci. 59, 1787–1802.

Kramer, I., Sigrist, M., de Nooij, J.C., Taniuchi, I., Jessell, T.M., Arber, S., 2006. A role for *Runx* transcription factor signaling in dorsal root ganglion sensory neuron diversification. Neuron 49, 379–393.

Lawson, S.N., 1992. Morphological and biochemical cell types of sensory neurons. In: Scott, S.A. (Ed.), Sensory Neurons. Oxford Univ. Press, New York, pp. 27–59.

Lawson, S.N., Biscoe, T.J., 1979. Development of mouse dorsal root ganglia: an autoradiographic and quantitative study. J. Neurocytol. 8, 265–274.

Levanon, D., Brenner, O., Negreanu, V., Bettoun, D., Woolf, E., Eilam, R., Lotem, J., Gat, U., Otto, F., Speck, N., Groner, Y., 2001. Spatial and temporal expression pattern of Runx3 (Aml2) and Runx1 (Aml1) indicates non-redundant functions during mouse embryogenesis. Mech. Dev. 109, 413–417.

Levanon, D., Bettoun, D., Harris-Cerruti, C., Woolf, E., Negreanu, V., Eilam, R., Bernstein, Y., Goldenberg, D., Xiao, C., Fliegauf, M., Kremer, E., Otto, F., Brenner, O., Lev-Tov, A., Groner, Y., 2002. The Runx3 transcription factor regulates development and survival of TrkC dorsal root ganglia neurons. EMBO J. 21, 3454–3463.

Lian, J.B., Balint, E., Javed, A., Drissi, H., Vitti, R., Quinlan, E.J., Zhang, L., Van Wijnen, A.J., Stein, J.L., Speck, N., Stein, G.S., 2003. Runx1/AML1 hematopoietic transcription factor contributes to skeletal development in vivo. J. Cell Physiol. 196, 301–311.

Marmigere, F., Montelius, A., Wegner, M., Groner, Y., Reichardt, L.F., Ernfors, P., 2006. The Runx1/AML1 transcription factor selectively regulates development and survival of TrkA nociceptive sensory neurons. Nat. Neurosci. 9, 180–187.

Molliver, D.C., Wright, D.E., Leitner, M.L., Parsadanian, A.S., Doster, K., Wen, D., Yan, Q., Snider, W.D., 1997. IB4-binding DRG neurons switch from NGF to GDNF dependence in early postnatal life. Neuron 19, 849–861.

Moqrich, A., Earley, T.J., Watson, J., Andahazy, M., Backus, C., Martin-Zanca, D., Wright, D.E., Reichardt, L.F., Patapoutian, A., 2004. Expressing TrkC from the TrkA locus causes a subset of dorsal root ganglia neurons to switch fate. Nat. Neurosci. 7, 812–818.

Okuda, T., van Deursen, J., Hiebert, S.W., Grosveld, G., Downing, J.R., 1996. AML1, the target of multiple chromosomal translocations in human leukemia, is essential for normal fetal liver hematopoiesis. Cell 84, 321–330.

Okada, H., Watanabe, T., Niki, M., Takano, H., Chiba, N., Yanai, N., Tani, K., Hibino, H., Asano, S., Mucenski, M.L., Ito, Y., Noda, T., Satake, M., 1998. AML1(−/−) embryos do not express certain hematopoiesis-related gene transcripts including those of the *PU.1* gene. Oncogene 17, 2287–2293.

Onodera, K., Takahashi, S., Nishimura, S., Ohta, J., Motohashi, H., Yomogida, K., Hayashi, N., Engel, J.D., Yamamoto, M., 1997. GATA-1 transcription is controlled by distinct regulatory mechanisms during primitive and definitive erythropoiesis. Proc. Natl. Acad. Sci. U. S. A. 94, 4487–4492.

Oppenheim, R.W., 1991. Cell death during development of the nervous system. Annu. Rev. Neurosci. 14, 453–501.

Patel, T.D., Jackman, A., Rice, F.L., Kucera, J., Snider, W.D., 2000. Development of sensory neurons in the absence of NGF/TrkA signaling in vivo. Neuron 25, 345–357.

Ritter, A.M., Lewin, G.R., Kremer, N.E., Mendell, L.M., 1991. Requirement for nerve growth factor in the development of myelinated nociceptors in vivo. Nature 350, 500–502.

Serbedzija, G.N., Fraser, S.E., Bronner-Fraser, M., 1990. Pathways of trank neral crest cell migration in the mouse embryo as revealed by vital dye labeling. Development 108, 605–612.

Simeone, A., Daga, A., Calabi, F., 1995. Expression of *runt* in the mouse embryo. Dev. Dyn. 203, 61–70.

Snider, W.D., McMahon, S.B., 1998. Tackling pain at the source: new ideas about nociceptors. Neuron 20, 629–632.

Stein, G.S., Lian, J.B., van Wijnen, A.J., Stein, J.L., Montecino, M., Javed, A., Zaidi, S.K., Young, D.W., Choi, J.Y., Pockwinse, S.M., 2004. Runx2/Cbfa1: a multifunctional regulator of bone formation. Oncogene 23, 4315–4329.

Suk-Chul, B., Joong-Kook, C., 2004. Tumor suppressor activity of RUNX3. Oncogene 23, 4336–4340.

Theriault, F.M., Roy, P., Stifani, S., 2004. AML1/Runx1 is important for the development of hindbrain cholinergic branchiovisceral motor neurons and selected cranial sensory neurons. Proc. Natl. Acad. Sci. 101, 10343–10348.

Theriault, F.M., Nuthall, H.N., Dong, Z., Lo, R., Barnabe-Heider, F., Miller, F.D., Stifani, S., 2005. Role for Runx1 in the proliferation and neuronal differentiation of selected progenitor cells in the mammalian nervous system. J. Neurosci. 25, 2050–2061.

Wang, Q., Stacy, T., Binder, M., Marin-Padilla, M., Sharpe, A.H., Speck, N.A., 1996. Disruption of the *Cbfa2* gene causes necrosis and hemorrhaging in the central nervous system and blocks definitive hematopoiesis. Proc. Natl. Acad. Sci. U. S. A. 93, 3444–3449.

Wassarman, P.M., DePamphilis, M.L., 1993. Guide to Techniques in Mouse Development. Academic Press, New York, NY.

Watson, A., Ensor, E., Symes, A., Winter, J., Kendall, G., Latchman, D., 1995. A minimal CGRP gene promoter is inducible by nerve growth factor in adult rat dorsal root ganglion neurons but not in PC12 phaeochromocytoma cells. Eur. J. Neurosci. 7, 394–400.

White, F.A., Silos-Santiago, I., Molliver, D.C., Nishimura, M., Phillips, H., Barbacid, M., Snider, W.D., 1996. Synchronous onset of NGF and TrkA survival dependence in developing dorsal root ganglia. J. Neurosci. 16, 4662–4672.

White, F.A., Keller-Peck, C.R., Knudson, C.M., Korsmeyer, S.J., Snider, W.D., 1998. Widespread elimination of naturally occurring neuronal death in Bax-deficient mice. J. Neurosci. 18, 1428–1439.

Yokomizo, T., Takahashi, S., Mochizuki, N., Kuroha, T., Ema, M., Wakamatsu, A., Shimizu, R., Ohneda, O., Osato, M., Okada, H., Komori, T., Ogawa, M., Nishikawa, S.-I., Ito, Y., Yamamoto, M., in press. Characterization of GATA-1^{+} hemangioblastic cells in the mouse embryo. EMBO J.

Yoshikawa, M., Ozaki, S., Noguchi, Y., Yokomizo, T., Takahashi, S., Senzaki, K., Shiga, T., 2005. Development of dorsal root ganglion neurons in Runx1-deficient mice. Abstr. - Soc. Neurosci. 35, 830.16.